HYDROLOGICAL PROCESSES
Hydrol. Process. **19**, 589–603 (2005)
Published online in Wiley InterScience (www.interscience.wiley.com). DOI: 10.1002/hyp.5609

Estimation of soil cracking and the effect on surface runoff in a Texas Blackland Prairie watershed

J. G. Arnold,[1]* K. N. Potter,[1] K. W. King[1] and P. M. Allen[2]

[1] *USDA-Agricultural Research Service, Temple, TX, USA*
[2] *Geology Department, Baylor University, Waco, TX, USA*

Abstract:

Seasonal cracking of the soil matrix results in poor estimates of runoff and infiltration by simulation models due to the changing soil storage conditions. In this study, soil surface elevation changes were measured every two weeks and soil crack volume was calculated for a two-year period at the USDA-Agricultural Research Service, Riesel Y-2 watershed in central Texas. Soil anchors were placed in triplicate at depths of 0·15, 0·45, 0·90, 1·50 and 2·5 m and relative movement from a monument at 4·5 m was measured. Soil movement was translated into crack volume assuming isotrophic shrinkage. A crack flow model was developed for this study that computes crack volume from crack potential, soil depth and soil moisture. Simulated crack volume followed the seasonal trends found in the measured crack volume and was in general agreement with a regression $R^2 = 0{\cdot}84$. The crack model was incorporated into SWAT (Soil and Water Assessment Tool), a comprehensive hydrologic model. Regression analysis was performed on measured and simulated daily surface runoff with an $R^2 = 0{\cdot}87$ indicating good agreement. The model was able to simulate surface runoff accurately in winter months when cracks were swelled closed and in the fall recharge events of 1998 when crack volume went from 70 to 10 mm. The relationships between measured crack volume and hydrologic variables simulated by the model were also examined and discussed. Copyright © 2005 John Wiley & Sons, Ltd.

KEY WORDS crack measurement; hydrologic model; vertisols; shrinking/swelling soils

INTRODUCTION

It is estimated that 320 million hectares of the world's land area is covered with expansive soils (Dudal and Eswaran, 1988) and up to 20% of the United States may be mantled with soils subject to shrink–swell behaviour (Krohn and Slosson, 1980). The consequences of shrink–swell behaviour of clay soils are mainly unfavourable for both agricultural and engineering uses. On the favourable side, some of these soils have higher water retention capacity. In non-agricultural use, shrink–swell behaviour results in significant damage to lightly loaded structures and roadways and enhances the probability of shallow slope failures (Anderson *et al*., 1982). In the United States, total damage due to shrink–swell is estimated to cost from 6 to 11 billion dollars per year (Nuhfer *et al*., 1993). In the Blackland Prairie of Texas, it is estimated to approach 100 million dollars a year (Allen and Maier, 1993). In agriculture, soil shrinkage cracking allows rapid transport of water, nutrients and pesticides to the subsoil where they are both inaccessible to shallow rooting plants and can pollute the local groundwater system (Kissel *et al*., 1974; Harris *et al*., 1994; Bronswijk *et al*., 1995; Kelly and Pomes, 1998). In addition, seasonal cracking of the soil matrix results in poor estimates of runoff and infiltration due to the changing soil storage conditions (Smettem *et al*., 1991; Stolte *et al*., 1997; Ruan and Illangasekare, 1998). In all cases, the prediction of the temporal change in soil volume is paramount to proper assessment of soil behaviour (Lin *et al*., 1998).

* Correspondence to: J. G. Arnold, USDA, ARS Grassland Soil and Water Research Lab, 808 East Blackland Road, Temple, TX 76502 USA. E-mail: jgarnold@spa.ars.usda.gov

Received 29 January 2002
Accepted 7 May 2004

The dynamic and highly complex behaviour of the infiltration and runoff process in expansive soil terrain is best studied in the field (Bouma and Loveday, 1988). However, such field studies of swelling and shrinking of clay soils are scarce owing to the lack of sound experimental methods and complementary mathematical equations (Bronswijk, 1991). Characterization of soil volume changes and related interaction with the soil water balance has been summarized by Bouma and Loveday (1988) and Bronswijk (1991). Previous attempts at modelling clay soil systems have proven difficult, with existing simulation models based on Darcy's law. This is not a valid assumption for preferential flow through non-capillary sized openings as shrinkage cracks (Beven and Germann, 1982). Newer models have been proposed which simulate infiltration at the soil surface with macropores (Hoogmoed and Bouma, 1980), flow in macropores and through the soil matrix with no volume changes (Beven and Germann, 1982), and models that attempt to do both (Germann and Beven, 1985; Jarvis and Leeds-Harrison, 1990; Bootlink *et al*., 1993; Gerke and van Genuchten, 1993; Hendricks *et al*., 1999; Larson and Jarvis, 1999). While these studies have proven successful in localized terrain, they require detailed characterization of macropore structure and soil properties with depth at each site. In addition, these studies have focused on assessing the short-circuiting of nutrients and pesticides and have not addressed long-term changes in soil runoff in such terrain.

Understanding and predicting runoff and storage (internal catchment) in swelling soils requires knowledge of the dynamic processes of soil cracking (Van Stiphout *et al*., 1987; Bronswijk, 1991). Studies by Jamison and Thompson (1967), Yaalon and Kalmar (1978), Bauer *et al*. (1993), Cheng and Pettry (1993) and Coquet (1998) have observed changes in layer thickness and crack volume during the year. Ritchie *et al*. (1972) assessed soil shrinkage/water content relationships in small and large cores. However, none of the studies have linked this assessment with either runoff or infiltration processes.

The objectives of this study are threefold: (1) to measure the hydrologic properties (storage or internal catchment) of fully cracked surface soils and to evaluate the effects of measurements on catchment discharge; (2) to make physical measurements of surface water runoff and crack volume; and (3) to model surface water runoff with a 'crack' subroutine.

MATERIALS AND METHODS

Experimental watershed

Watershed Y-2 located at the USDA-ARS research site in Riesel, TX was selected as the study site. The USDA-ARS Riesel watersheds are located in the heart of the Blackland Prairie. The Blackland Prairie is a stretch of fertile agricultural lands extending from San Antonio in the south to the Red River in the north.

Watershed Y-2 (Figure 1) drains 53·4 ha and is comprised of four nested subwatersheds. The dominant soils in the watershed are Houston Black (fine, montmorillonitic, thermic, udic Haplustert) soils, which exhibit a strong potential for shrinking and swelling. The composition of the Houston Black soil is 17·2% sand, 27·8% silt and 55·0% clay, and is classified by the USDA as D type soil. The saturated conductivity associated with the Houston Black series is 1·52 mm h^{-1}. The slopes are generally 1–3% and classified as gently rolling. The 60-year mean annual rainfall is approximately 850 mm. Present-day land use in the watershed is a mixture of cropping (corn, sorghum and oats) and pasture systems (Table I). A full spectrum of tillage and management operations are used throughout the watershed. Precipitation, runoff and groundwater levels are monitored continuously and connected via a telemetric network.

Crack measurements

Shallow soil anchors were placed in triplicate at depths of 0·15 m and 0·45 m. Deeper borros point (heave settlement) anchors were installed at 0·90, 1·5 and 2·5 m. In each case, the anchor was separated from the surrounding soil by a collar so as to prevent any movement above the anchor influencing the measurements. The monument was installed below dry period water table (4·5 m). This consisted of an iron bar which was

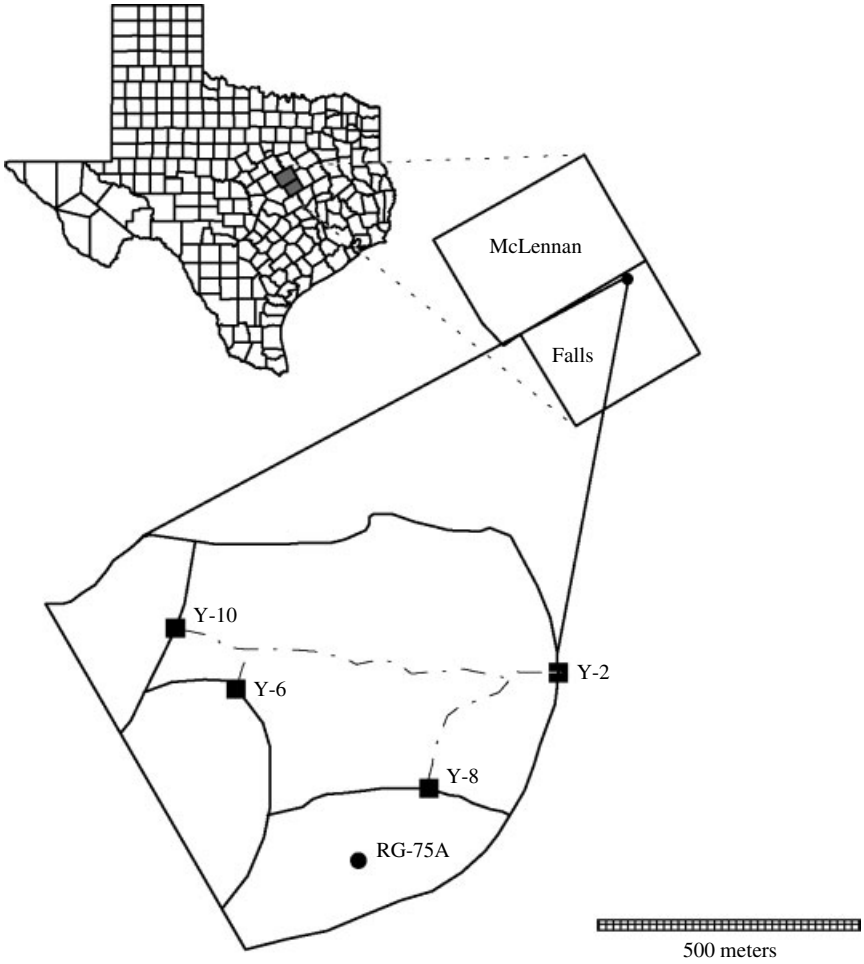

Figure 1. Location of ARS experimental watershed near Riesel, TX

cemented into the weathered rock and then provided with a collar to the surface (Figure 2). Measurements were made every two weeks using a surveyor's level and stadia rod. Measurements were made to the nearest 3 mm. The maximum distance from the transit to the anchors was about 6 m. In addition to monitoring the soil swell, rainfall and runoff was monitored at the site using an array of five continuous tipping bucket samplers and multiple calibrated weirs for surface flow.

Crack volume per unit area (V_{cr}) is estimated from changes in layer thickness after Bronswijk (1991) and Bauer *et al*. (1993):

$$\Delta V = (1 - (1 - \Delta Z/Z)^3)Z \tag{1}$$

$$V_{cr} = \Delta V - \Delta Z \tag{2}$$

where Z is layer thickness (mm), ΔZ is change in layer thickness (mm) and ΔV is change in crack volume per unit area (mm).

Table I. Management practices for nested watersheds of Y-2* at Riesel, TX

Date	Y-6	Y-8	Y-10
4-Mar-98	—	—	cultivator
28-Mar-98	—	—	plant corn
17-Apr-98	—	—	cultivator
23-May-98	harvest oats	harvest wheat	—
2-Jun-98	—	disk till	—
4-Jun-98	disk till	—	—
7-Jul-98	disk till	—	—
8-Jul-98	—	disk till	—
30-Jul-98	—	—	harvest corn
24-Aug-98	disk till	disk till	—
22-Sep-98	disk till	—	—
23-Sep-98	—	disk till	—
19-Jan-99	cultivator	cultivator	—
20-Jan-99	—	—	cultivator
17-Feb-99	cultivator	cultivator	cultivator
23-Mar-99	—	plant sorghum	plant sorghum
24-Mar-99	cultivator	—	—
26-Mar-99	plant sorghum	—	—
3-Aug-99	—	—	harvest sorghum
5-Aug-99	harvest sorghum	harvest sorghum	—
13-Aug-99	—	—	disk till
23-Aug-99	disk till	disk till	disk till
4-Oct-99	—	—	disk till
5-Oct-99	disk till	—	—
7-Oct-99	—	disk till	—
26-Oct-99	disk till	disk till	—
27-Oct-99	—	—	sweep chisel
8-Nov-99	disk till	—	cultivator
9-Nov-99	—	—	plant wheat
10-Nov-99	plant oats	—	—
16-Nov-99	—	sweep chisel	—

* Management of remainder of watershed Y-2 consisted of pasture for the study period.

Hydrologic model

The influence of cracks on runoff and recharge was investigated using the Soil and Water Assessment Tool (SWAT) model (Arnold *et al*., 1998). SWAT is a complex, conceptual model with spatially explicit parameterization. It is a continuous time model that operates on a daily time step. The objective in model development was to predict the impact of management on water, sediment and agricultural chemical yields in ungauged basins. To satisfy the objective, the model: (a) is physically based (calibration is not possible on ungauged basins); (b) uses readily available inputs; (c) is computationally efficient to operate on large basins in a reasonable time; and (d) is in continuous time and capable of simulating long periods for computing the effects of management changes. Major model components include: weather, hydrology, soil temperature, plant growth, nutrients, pesticides and land management. A brief description of the hydrology/water balance is given here and a complete description of model components is found in Arnold *et al*. (1998). The water balance of each hydrologic response unit (HRU) in the watershed is represented by four storage volumes: snow, soil profile (0–2 m), shallow aquifer (typically 2–20 m) and deep aquifer (>20 m). In this study, the HRU is defined as unique combinations of land use and soil. The soil profile can be subdivided into multiple layers. Soil water processes include infiltration, evaporation, plant uptake, lateral flow and percolation to lower layers. Excess rainfall is calculated using the Green–Ampt Mein–Larson infiltration method (King and

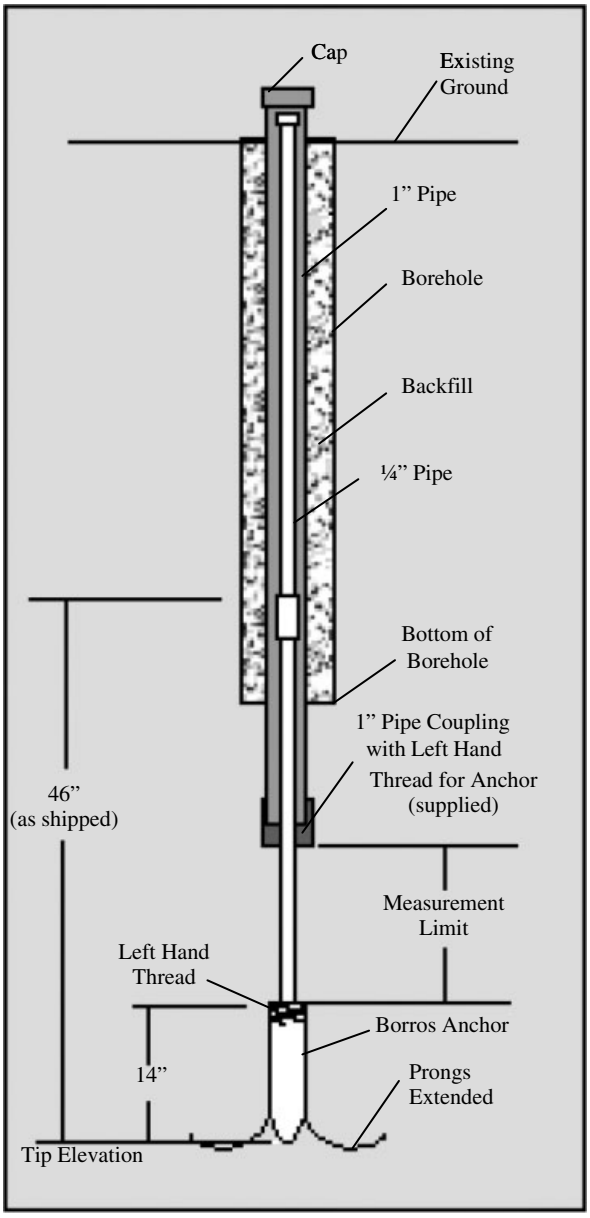

Figure 2. Diagram for installation of borros anchors

Arnold, 1999). Percolation from the bottom of the soil profile recharges the shallow aquifer. Shallow aquifer components include evaporation, pumping withdrawals and seepage to the deep aquifer.

Crack submodel

The crack flow submodel was developed for this study and incorporated into SWAT. Potential crack volume is simulated for each soil layer with the equation

$$CD_{pot} = C_{pot}\, e^{(-0{\cdot}0012d)}\, Z \tag{3}$$

where CD_{pot} is potential crack volume for the soil layer as a function of depth (mm), C_{pot} is the potential crack volume of the soil layer (fraction input to the model), d is the depth to the middle of the soil layer (mm) and Z is the thickness of the layer (mm). Soil movement is related to both seasonal moisture changes and overburden pressure (Bronswijk, 1991). The depth of the active zone or depth of desiccation is defined as the thickness of the layer where a soil moisture deficiency exists. This is a transient zone and influenced by the soil type, soil structure, climate and topography. The two parameters, which must be defined in a study of swelling of soils, are the depth of the active zone and the seasonal change of soil moisture with depth. Plots of soil suction with depth based on field and laboratory derived suction measurements are often used to assess the depth at which the equilibrium suction (active depth) is reached according to the Russam Coleman curves (Bryant, 1999; Russam and Coleman, 1961). The depth of changes in soil moisture and suction in Bryant's study extended to 6 m. Most of the reported variation occurred in the top 4 m. Wise and Hudson (1971) indicate that the common depth of active swelling in Texas is slightly less than 2 m. At the study site in Riesel, soil suction was computed (ASTM D5298-93) during the fall of 1999. Soil suction decreases with depth and reaches an equilibrium suction around 2–3 m. At the Riesel test site, this depth is about 0·3 m above the seasonally high water table depth and is thought to represent the capillary zone.

The range of soil moisture variation with depth and hence potential for swelling or cracking is the second parameter. This factor accounts for the exponential decay with depth ($e^{(-0.0012d)}$) given in Equation (3). In this study, this parameter was calculated using an adaptation of the volume change factor after Davis and Tucker (1973) and McKeen and Hamberg (1992). The volume change factor is a function of site soil moisture changes with depth, overburden pressure and swell potential of the soil. The volume change factor is defined such that this factor is 1 at a depth of 0·3 m and <1 for deeper depths, as shown in Figure 3.

The moisture levels used in this function were calculated based on field measurements of soil moisture with depth in the Dallas Fort Worth area over an 18-month period (Davis and Tucker, 1973). The percentage swell/moisture content relationships were defined using both free swell tests and swell pressure tests (Davis and Tucker, 1973). Since the soil (clay types) and bedrock at the test site and that used by Davis and Tucker are similar, the volume change factor curve with depth was thought appropriate for the Riesel test site. While this procedure relies on localized moisture data and laboratory tests, a similar relationship can be obtained with knowledge of the soil's plasticity index, cation exchange capacity and percentage passing the #200 sieve (Wray, 1997). Wray shows a methodology to calculate the maximum soil suction changes over the season with depth.

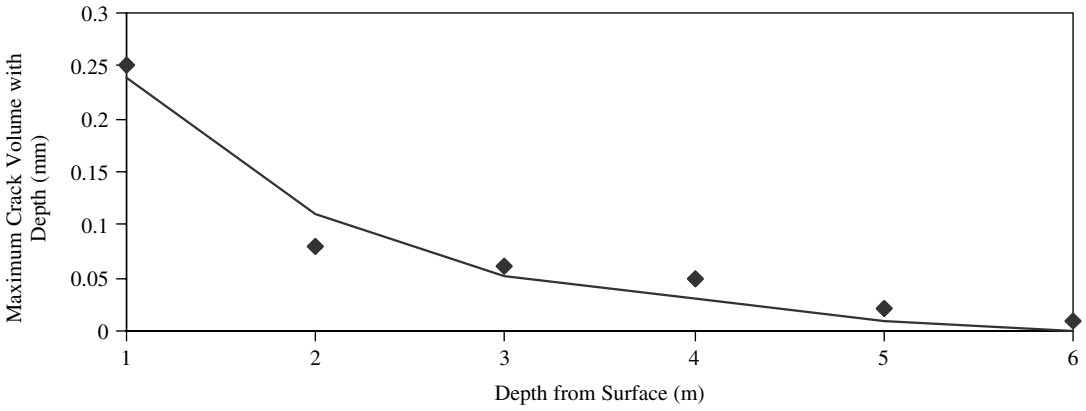

Figure 3. Relationship between maximum crack volume and depth below the soil surface

Soil moisture adjustment. Actual crack volume is updated daily for each layer in the model according to the equation

$$\mathrm{CV} = \mathrm{CD}_{\mathrm{pot}} * (\mathrm{fc} - \mathrm{sw})/\mathrm{fc} \tag{4}$$

where CV is actual crack volume (mm), fc is field capacity of the soil layer (mm) and sw is the current soil water content of the layer (mm). Three benchmark points have been established in clay behaviour: (1) the intercept at zero water content is found consistently at 174 385 kPa (6·25 pF); (2) the suction level at which volume change ceases is about 31 010 kPa (5·5 pF), or the soil's shrinkage limit; and (3) the volume change ceases at field capacity in the range of 9·8–31 kPa (2–2·5 pF) (McKeen, 1992). In addition, the soil suction/volume change curve can be approximated as a straight line between field capacity and the shrinkage limit of the soil, enabling the above relationship [Equation (4)] to be used.

Lagging crack volume expansion. Crack volume is lagged according to the equation

$$\mathrm{CV}_{\mathrm{lag}} = \rho\ \mathrm{CV}_{i-1} + (1 - \rho)\mathrm{CV}_i \tag{5}$$

where $\mathrm{CV}_{\mathrm{lag}}$ is the crack volume adjusted for lag, ρ is the diffusion coefficient, CV_{i-1} is the crack volume on the previous day, CV_i is the crack volume on the current day and i is the current day. Lagging is allowed to occur only during drying and when size sw $<$0·9 fc. The rate of diffusion of moisture under suction changes is the diffusion coefficient of the soil and is analogous to the coefficient of consolidation in classical consolidation theory (Mitchell, 1980). Upon drying, soil moisture redistribution within the profile (lag) is considered to be a function of the diffusion coefficient (Mitchell, 1980). While water entry into the soil is driven predominantly by hydraulic forces, water leaving the soil below the wilting point is related to the diffusion coefficient. This value can be calculated: (1) in the laboratory; (2) in the field based on analysis of soil moisture variations with depth over time (McKeen and Johnson, 1990); and (3) from analysis of well level declines in the active zone over time. Since estimates of the drainable porosity and diffusivity are difficult without extensive laboratory tests or field measurements, available field measurements of well heights over time were used to calculate the lag in this study.

The α factor is calculated from the decline in well levels using the equation (Arnold *et al.*, 1995)

$$\alpha = 2{\cdot}3\ \ln(h_1 - h_2)/t \tag{6}$$

where α is the well recession constant, h_1 is the well height at time zero and h_2 is the well height at time t. The diffusion coefficient ρ is related to α by the equation

$$\rho = \exp(-\alpha) \tag{7}$$

Analysis of well heights near the crack measurements yielded an α value of 0·015. This corresponds to a ρ of 0·985, which was used in this study.

Surface runoff and soil water routing. Surface runoff is computed by the model and then adjusted for crack volume:

$$\mathrm{qd}_{\mathrm{c}} = \mathrm{qd} - \mathrm{CV}_{\mathrm{tot}} \tag{8}$$

where qd_{c} is surface runoff adjusted for cracks (mm), qd is surface runoff as computed by the model (mm) and $\mathrm{CV}_{\mathrm{tot}}$ is total crack volume for the entire soil profile (sum of all layers, mm). In Equation (8), qd is computed using the Green and Ampt infiltration equation (King and Arnold, 1999) without taking cracks into account (using the saturated conductivity of the soil matrix). Percolation from one soil layer to the next is also adjusted for crack volume. Water that infiltrates (I) is calculated by:

$$I = P - \mathrm{qd}_{\mathrm{c}} \tag{9}$$

where P is rainfall amount (mm). Infiltrated water is first allowed to fill the crack volume starting in the lowest soil layer and proceeding to the surface. All water that flows into the cracks is assumed to accumulate at the bottom of the cracks and is added to the soil moisture of the corresponding soil layers after Hendricks *et al*. (1999).

Simulation approach

The hydrologic components of the model have been validated for numerous watersheds (Arnold and Allen, 1996) and a comprehensive validation of stream flow was performed for the entire coterminous USA (Arnold *et al*., 1999). The Riesel watersheds were one of the original validation sites for the SWAT model and its predecessor models (Arnold and Williams, 1987) and thus had inputs developed for Riesel watershed Y-2. In this study, SWAT was run without further calibration. The crack flow subroutines were then added to the model and simulated crack volume and runoff were compared against measured values.

Watershed inputs. The watershed was subdivided to account for differences in topography and land use (Figure 1). Soil layers were set to coincide with the crack measurement depths. Houston Black is the dominant soil series and was used in all four subwatersheds. Required soil properties were obtained from the Soils-5 database (USDA Soil Conservation Service, 1992). Breakpoint precipitation and daily maximum and minimum temperature were recorded at RG-75A (Figure 1). Management operations were simulated as shown in Table I and plant-specific growth parameters were taken from a database supplied with the model (Arnold *et al*., 1998).

RESULTS AND DISCUSSION

Observed soil movement and crack volume

Soil movement was monitored biweekly beginning in January 1998. Figure 4 illustrates the relative movement of soil anchors at 0·15, 0·45, 0·90, 1·5 and 2·4 m below ground surface relative to the deep borros point monument at 4·5 m. Movement was set to zero at the beginning of measurements in January 1998, with increasing positive movement indicating the anchors are moving farther from the monument (swelling) and decreasing movement indicating the anchors are moving closer to the monument (shrinkage). Several observations can be made from the monument data. The annual magnitude of movement relative to the monument (shrinkage and swelling of soil) is inversely related to soil depth. The maximum crack volume was 78 mm over the 4·5 m depth to the monument. Over 70% of the crack volume was found in the upper 1·5 m. Maximum movement of the 0·15 m anchor is 82 mm, while the maximum movement at 2·4 m is 15 mm.

Total crack volume was computed from soil movement using Equations (1) and (2) for each layer and then summed for the entire soil profile. Figure 5 shows measured estimates of total crack volume at two-week intervals. The measured crack volume is closely related to the movement of the 150 mm anchor, which would be an indicator of total crack volume.

Validation of crack volume

Model prediction of total soil profile crack volume during 1998 and 1999 is compared against measured volumes in Figure 5. Daily model output is shown as a solid line while measured crack volumes are shown as points every two weeks. Seasonal weather conditions in 1998 and 1999 were similar—a wet winter and early spring followed by a dry summer and fall with high potential for cracking. Reasonable agreement was obtained to day 100 (January to April), then the model predicted opening of cracks at a faster rate than observed in the field. A value of 0·985 was used for ρ in Equation (5) to lag the expansion of cracks as drying occurred. During wetting between days 250 and 300 (September–November 1998), crack volume closed rapidly as the soil wets and swells, which the model simulated accurately. However, the cracks tend to close and remain closed during the winter months while the model allows the cracks to open and close rapidly (days 350–500). Regression analysis was performed on the measured and simulated crack volumes on days when measurements were taken (49 points). Regression yielded

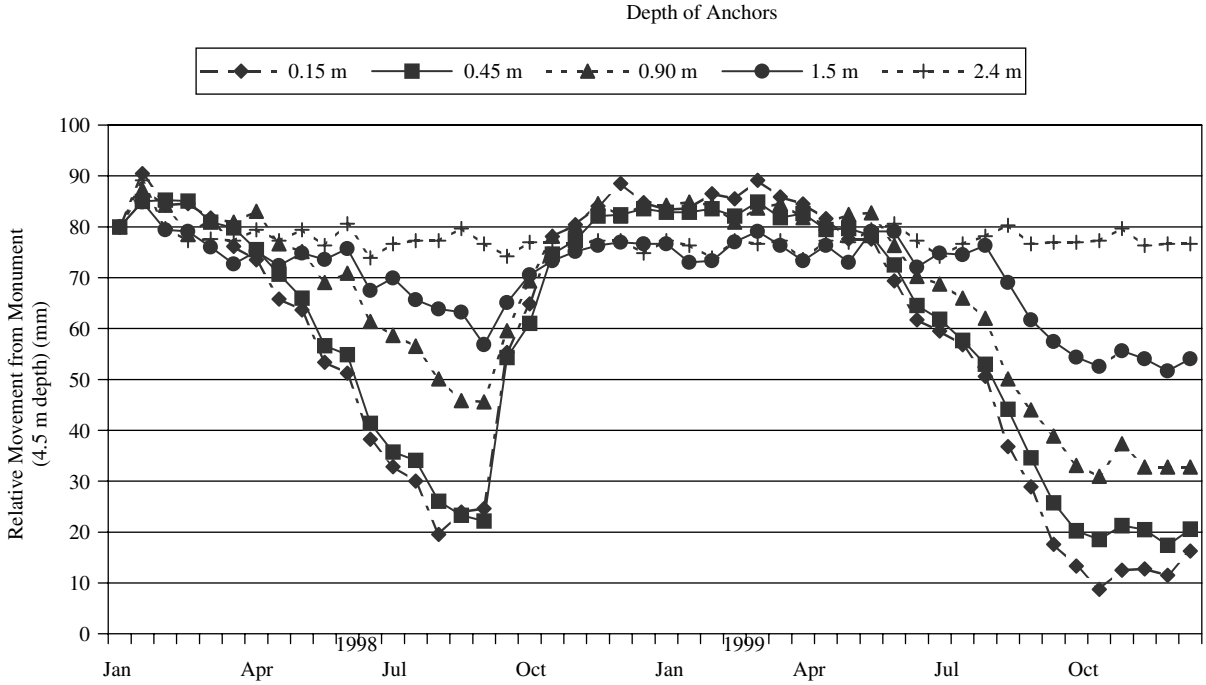

Figure 4. Movement of borros anchors relative to the monument at 4·5 m depth

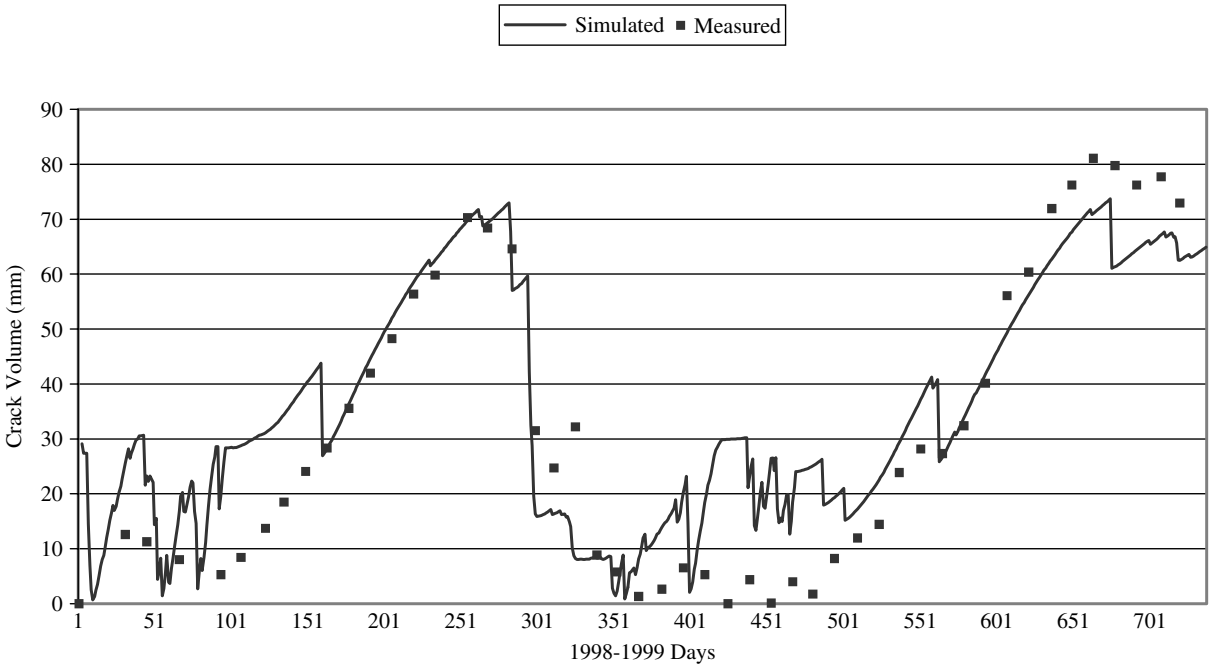

Figure 5. Measured and simulated total crack volumes for 1998–1999

an R^2 of 0·84, indicating the model presented in this study was able to realistically simulate crack volume.

Validation of surface runoff

The model was run with four subwatersheds as shown in Figure 1. Subwatersheds Y-6, Y-8 and Y-10 were tilled (Table I) and the potential crack volume (C_{pot}) was set at 2% assuming that many of the cracks are closed by tillage. The remainder of watershed Y-2 is pasture, without tillage to close the cracks, and C_{pot} was set to 6%. Figures 6 and 7 show daily time series of runoff for the entire watershed that outlets at station Y-2. Most events compare reasonably well. Some are overpredicted and some underpredicted, but no general tendencies are evident. Figure 8 is a daily regression plot of measured and simulated runoff. The R^2 value is 0·87 and the regression slope is near one, indicating a reasonable fit. There were 66 measurable rainfall events during the 1998–1999 period. Total precipitation was 1318 mm with measured runoff of 228 mm and simulated runoff of 245 mm.

Relationship between crack volume and hydrologic variables

It is of interest to observe the relationship of measured crack volume and hydrologic variables in the model. The relationship between crack volume and simulated soil water is shown in Figure 9. There is a direct inverse relationship, which is explained by Equation (4). The lag between soil water and crack volume is evident in Figure 9. Soil water has already fallen below 25 mm before day 150, while crack volume is just beginning to increase and does not peak until day 250, when soil water is already beginning to rise. Throughout the winter and spring, soil water remains high and crack volume low. Soil water decreases sharply during the growing season (days 475–525) and crack volume does not begin to increase until day 550. The increase continues throughout the fall of 1999 as soil water remains relatively low.

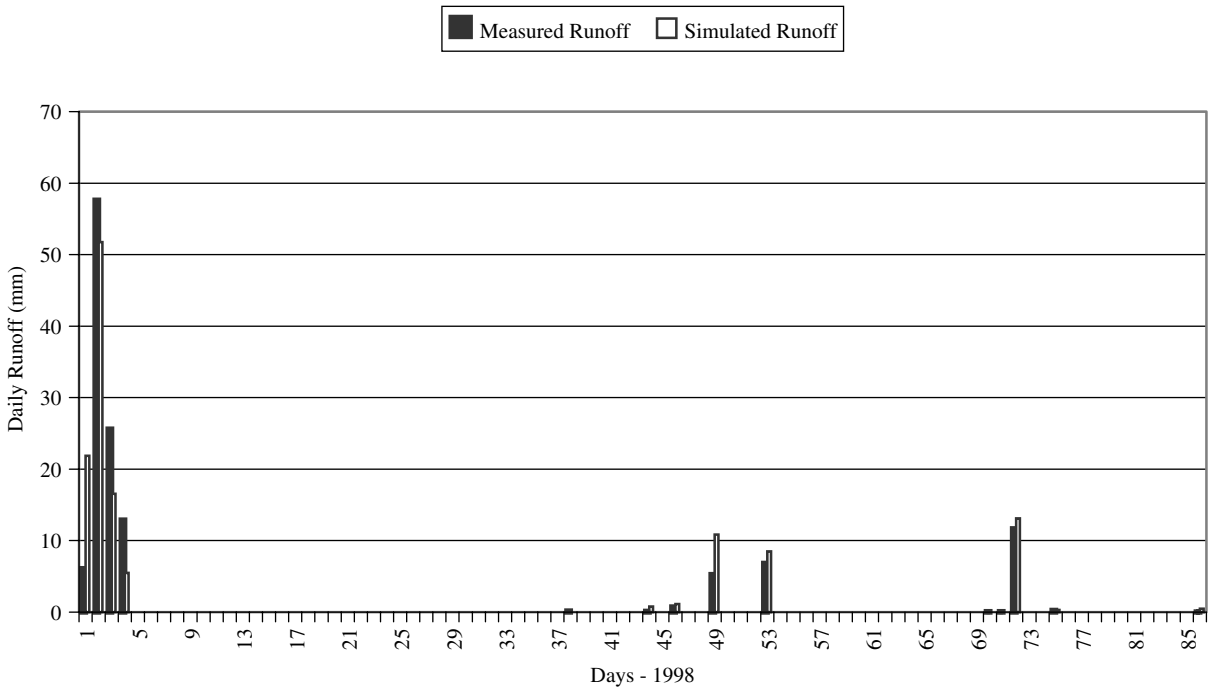

Figure 6. Measured and simulated daily surface runoff for all events during Julian days 1–86, 1998

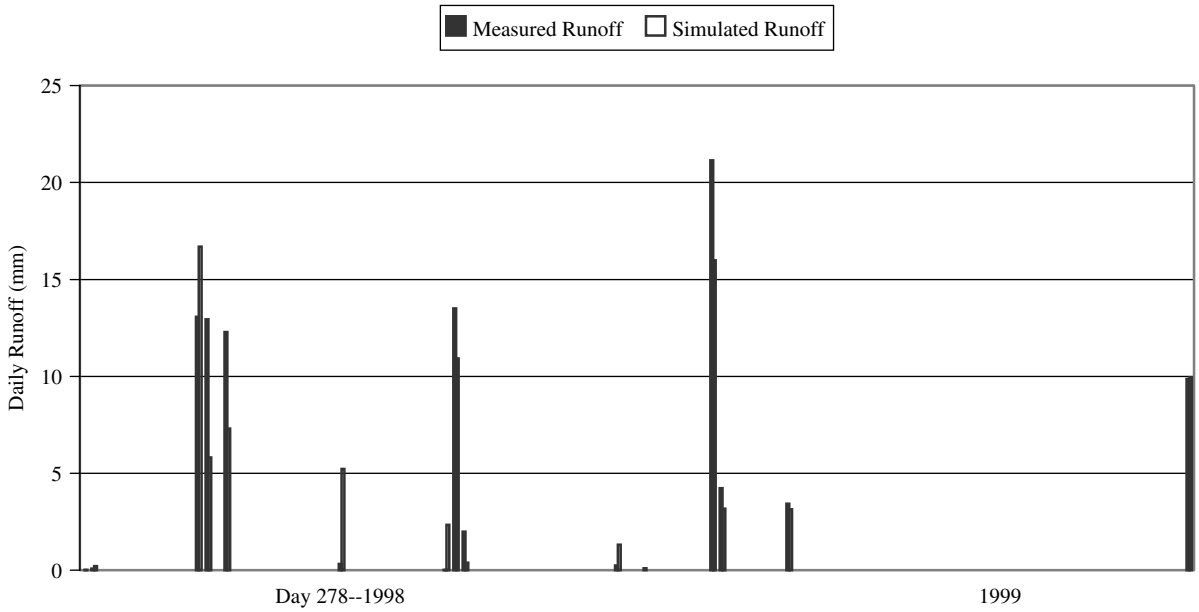

Figure 7. Measured and simulated daily surface runoff for all events during Julian days 278, 1998 through 365, 1999

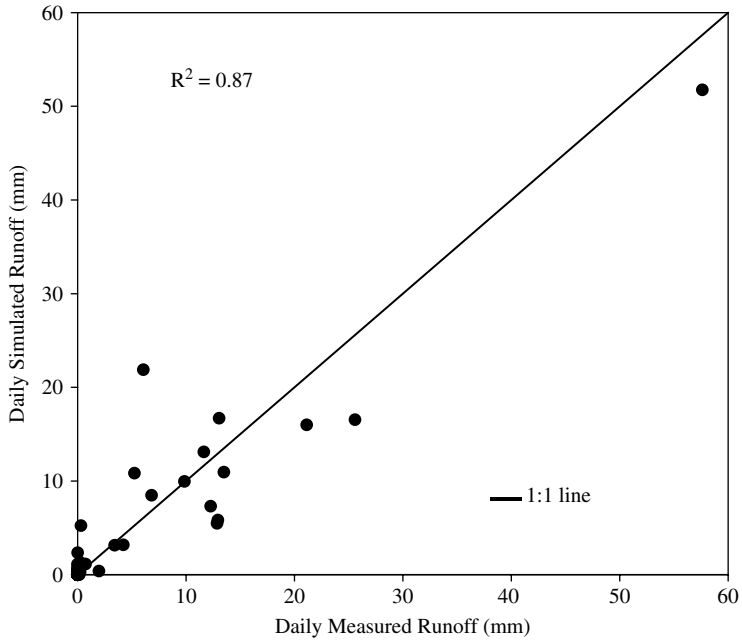

Figure 8. Daily regression plot of measured and simulated daily runoff

Crack volume and potential evapotranspiration (PET) have similar distributions, however, crack volume lags PET by approximately three months (Figure 10). Obviously there is a strong interdependence of PET on soil water, with soil water being inversely related to PET. Actual evapotranspiration (AET) has a far different relationship to crack volume than PET (Figure 11). There is also about a three-month lag between

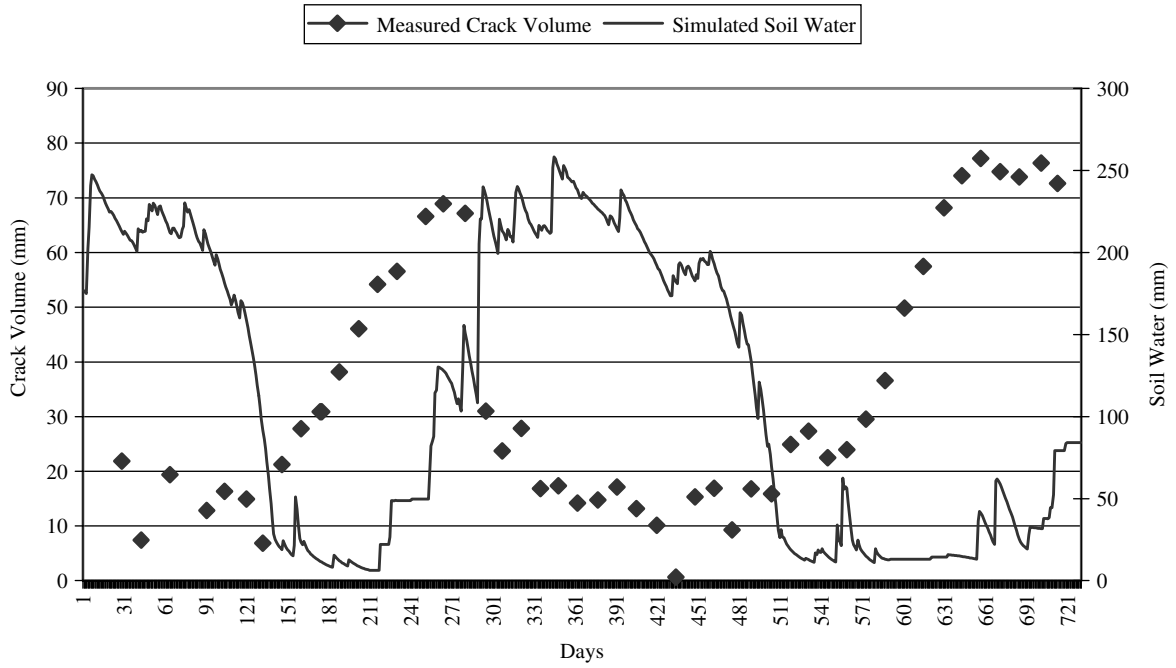

Figure 9. Relationship between crack volume and simulated soil water

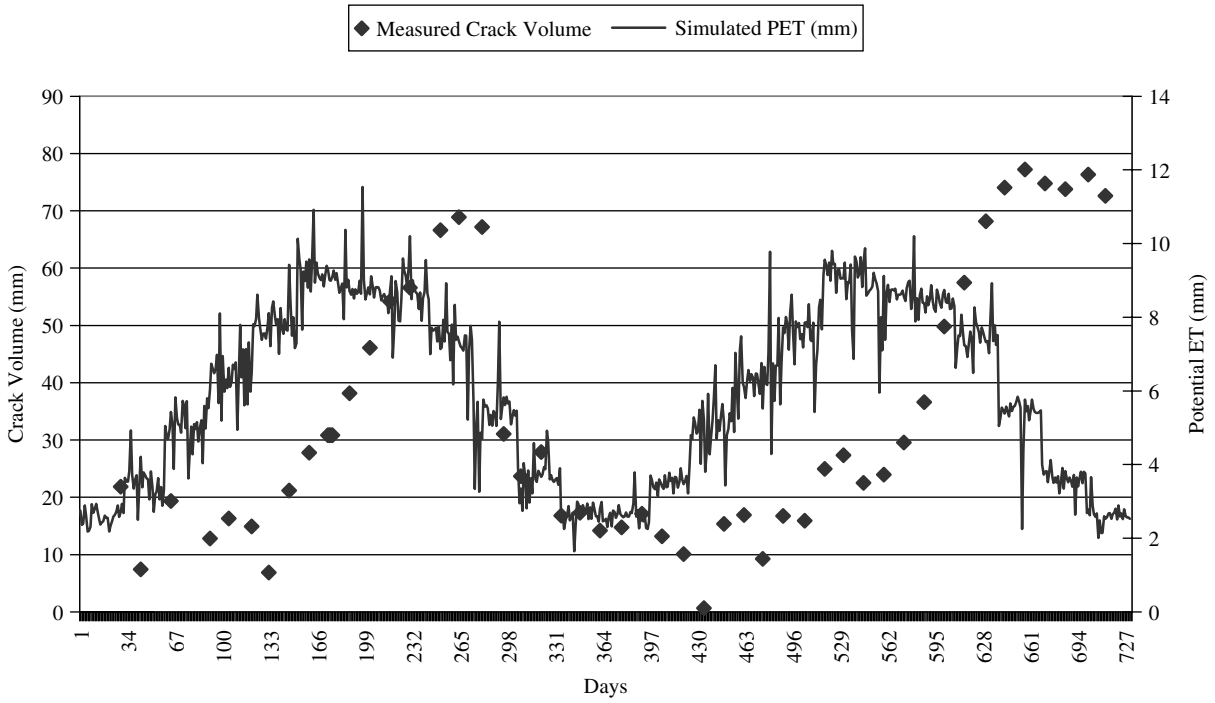

Figure 10. Relationship between crack volume and simulated potential evapotranspiration

peak AET and peak crack volume. AET decreases dramatically in the summer when soil water is depleted. The relationship between simulated runoff and crack volume is given in Figure 12. Runoff occurs during rainfall events that also produce infiltration and an increase in soil water. In this example, runoff also occurs in the winter of both 1998 and 1999 in periods of low PET and low crack volumes.

SUMMARY AND CONCLUSIONS

Shrink–swell behaviour results in significant damage to lightly loaded structures and roadways and enhances the probability of shallow slope failures, with total damage estimated to cost from 6 to 11 billion dollars per year in the USA. Seasonal cracking of the soil matrix results in poor estimates of runoff and infiltration due to the changing soil storage and allows rapid transport of water, nutrients and pesticides to the subsoil where they can pollute the local groundwater system.

In this study, several observations were made from the monitored crack data including: (1) differential movement of 82 mm in a total depth of 4·5 m measured over a 24-month period in a vertisol overlying a calcareous shale; (2) maximum crack volume computed of 78 mm over 4·5 m; (3) crack volume changed with depth—over 70% of the crack volume was computed in the top 1·5 m; (4) crack volume changed seasonally, reaching a maximum in late fall and a minimum during winter; and (5) crack volume was greater during the second drought season. A crack volume model was developed under the following assumptions: (1) crack volume was modelled based on layer thickness changes due to calculated changes in soil moisture; (2) crack volume decreased with depth due to rooting depth and overburden pressure; and (3) crack volume lagged computed soil moisture changes in the model.

Simulated crack volume followed the seasonal trends found in the measured crack volume and was in general agreement with a regression $R^2 = 0{\cdot}84$. The crack model was incorporated into SWAT, a comprehensive

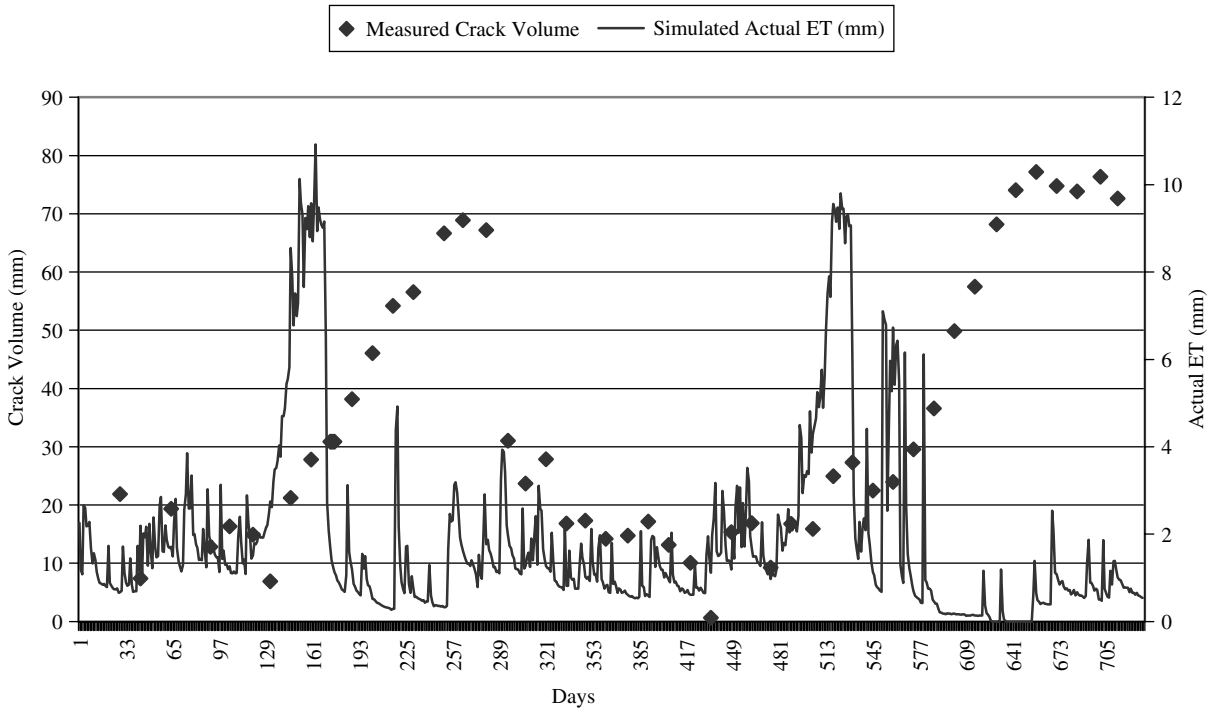

Figure 11. Relationship between crack volume and simulated actual evapotranspiration

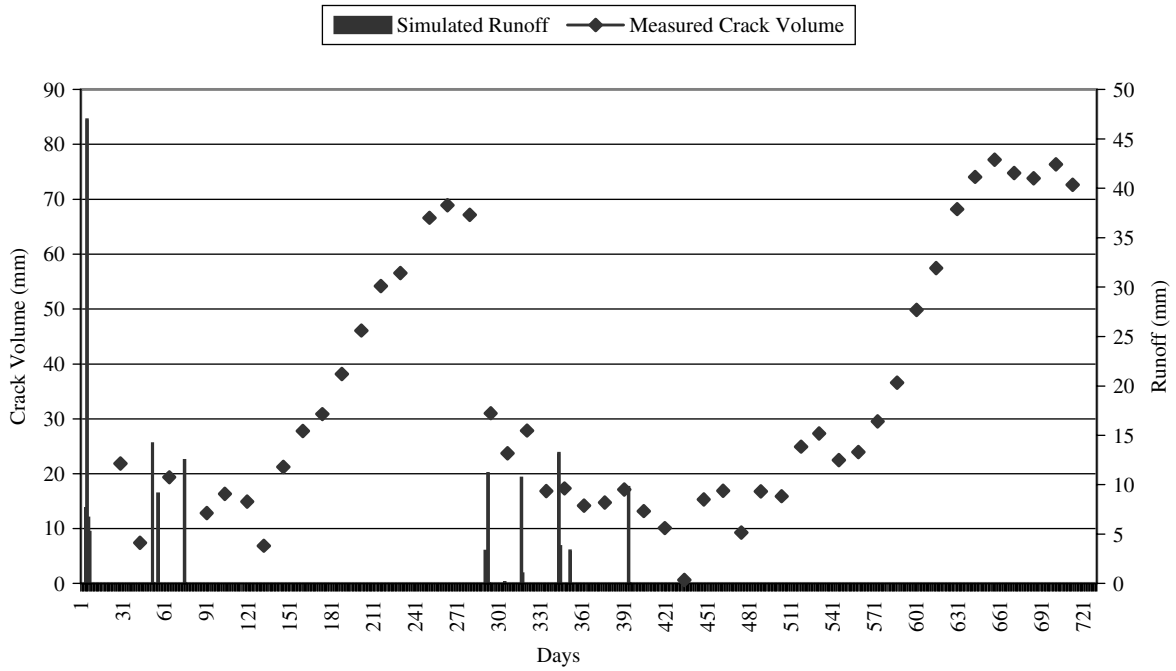

Figure 12. Relationship between crack volume and simulated surface runoff

hydrologic model. Regression analysis was performed on measured and simulated daily surface runoff with an $R^2 = 0{\cdot}87$ indicating good agreement. The model was able to simulate surface runoff accurately in winter months when cracks were swelled closed and in the fall recharge events of 1998 when crack volume went from 70 to 10 mm. The relationships between measured crack volume and hydrologic variables simulated by the model were also examined and discussed. Future research is planned to determine the impact of cracking on groundwater recharge and contaminant transport.

REFERENCES

Allen PM, Maier N. 1993. Growing cities: impacts of urbanization in the Blackland Prairie. In *The Texas Blackland Prairie: Land, History, Culture*, Sharpless M, Yelderman J (eds). Baylor University Press: Waco, TX; 237–251.

Anderson MG, Hubbard MG, Kneale PE. 1982. The influence of shrinkage cracks on pore pressure within a clay embankment. *Quarterly Journal of Engineering Geology London* **15**: 9–14.

Arnold JG, Allen PM. 1996. Estimating hydrologic budgets for three Illinois watersheds. *Journal of Hydrology* **176**: 55–77.

Arnold JG, Williams JR. 1987. Validation of SWRRB—simulator for water resources in rural basins. *Journal of Water Resources Planning and Management, ASCE* **113**(2): 243–256.

Arnold JG, Allen PM, Muttiah RS, Bernhardt G. 1995. Automated base flow separation and recession analysis techniques. *Groundwater* **33**(6): 1010–1018.

Arnold JG, Srinivasan R, Muttiah RS, Williams JR. 1998. Large area hydrologic modeling and assessment. Part I. Model development. *Journal of the American Water Resources Association* **34**(1): 73–89.

Arnold JG, Srinivasan R, Muttiah RS, Allen PM, Walker C. 1999. Continental scale simulation of the hydrologic balance. *Journal of the American Water Resources Association* **35**(5): 1037–1052.

Bauer JU, Anderson SH, McGinty KS. 1993. *Quantifying desiccation cracking in a Missouri claypan soil*. Agricultural Research to Protect Water Quality, Soil and Water Conservation Society; Minnesota; 378–381.

Beven K, Germann P. 1982. Macropores and water flow in soils. *Water Resources Research* **18**: 1311–1325.

Bootlink HWG, Hatano R, Bouma J. 1993. Measurement and simulation of bypass flow in a structured clay soil: a physico-morphological approach. *Journal of Hydrology* **148**: 149–168.

Bouma J, Loveday J. 1988. Characterizing soil water regimes in swelling clay soils. In *Vertisols: Their Distribution, Properties, Classification, and Management*, Wilding LP, Puentes R (eds). Texas A&M Press: College Station, TX; 83–96.

Bronswijk H. 1991. *Magnitude, modeling and significance of swelling and shrink processes in clay soils*. Staring Centrum Wageningen.

Bronswijk JJB, Hamminga W, Oostindae K. 1995. Field scale solute transport in a heavy clay soil. *Water Resources Research* **31**: 517–526.
Bryant JT. 1999. *Variation of soil suction with depth in Dallas, Fort Worth, Texas*. Transactions Research Record 100–104.
Cheng Y, Pettry DE. 1993. Horizontal and vertical movements of two expansive soils in Mississippi. *Soil Science Society of America Journal* **57**: 1542–1547.
Coquet Y. 1998. In situ measurement of the vertical linear shrinkage curve of soils. *Soil and Tillage Research* **46**: 289–299.
Davis RC, Tucker R. 1973. *Soil moisture and temperature variation beneath a slab barrier on expansive clay*. Report TR-5-73, Construction Research Center, University of Texas, Arlington.
Dudal R, Eswaran H. 1988. Distribution, properties, and classification of vertisols. In *Vertisols: Their Distribution, Properties, Classification, and Management*, Wilding LP, Puentes R (eds). Texas A&M Press: College Station, TX; 1–22.
Gerke HH, van Genuchten MT. 1993. A dual-porosity model for simulating the preferential movement of water and solutes in structured porous media. *Water Resources Research* **29**(2): 305–320.
Germann PF, Beven K. 1985. Kinematic wave approximation to infiltration into soils with sorbing macropores. *Water Resources Research* **21**(7): 990–996.
Harris GL, Nicholls PH, Bailey SW, Howse KR, Mason DJ. 1994. Factors influencing the loss of pesticides in drainage from a cracking clay soil. *Journal of Hydrology* **159**: 235–253.
Hendricks RFA, Oostindae K, Hamminga P. 1999. Simulation of bromide tracers and nitrogen in a cracked clay soil with FLOCR/ANIMO model combination. *Journal of Hydrology* **215**: 94–115.
Hoogmoed WB, Bouma J. 1980. A simulation model for predicting infiltration into cracked clay soils. *Soil Science Society of America Journal* **44**: 458–461.
Jamison VC, Thompson GA. 1967. Layer thickness changes in a clay-rich soil in relation to water content changes. *Soil Science Society of America Journal* **31**: 441–444.
Jarvis NJ, Leeds-Harrison PB. 1990. Field test of a water balance model of cracking clay soils. *Journal of Hydrology* **112**: 203–218.
Kelly BP, Pomes ML. 1998. Preferential flow and transport of nitrate and bromide in a claypan soil. *Ground water* **36**(3): 484–494.
King KW, Arnold JG. 1999. Comparison of Green–Ampt and curve number methods on Goodwin creek watershed using SWAT. *Transactions of the ASAE* **42**(4): 919–925.
Kissel DE, Ritchie JT, Burnett E. 1974. Nitrate and chloride leaching in a swelling soil. *Journal of Environmental Quality* **3**(4): 401–404.
Krohn JP, Slosson JE. 1976. Landslide potential in the United States: California. *Geology* **29**: 224–231.
Krohn JP, Slosson JE. 1980. Assessment on expansive soils in the United States. In *Proceedings of the 4th International Conference on Expansive Soils*, Denver, CO, Snethen D (ed.); 596–608.
Larson MH, Jarvis NJ. 1999. Evaluation of a dual porosity model to predict field scale solute transport in a macroporous soil. *Journal of Hydrology* **215**: 153–171.
Lin HS, McInnes KJ, Wilding LP, Hallmark CT. 1998. Macroporosity and initial moisture effects on infiltration rates in vertisols and vertic intergrades. *Soil Science* **163**(1): 2–8.
McKeen RG. 1992. A model for predicting expansive soil behavior. In *Proceedings of International Conference on Expansive Soils, ASCE* **1**: 1–6.
McKeen RG, Hamberg DJ. 1992. *Characterization of expansive soils*. Transportation Research Record 790, Transportation Research Board, National Academy of Science: Washington, DC; 76 pp.
McKeen RG, Johnson LD. 1990. Climate controlled soil design parameters for mat foundations. *Journal of Geotechnical Engineering, ASCE* **116**(7): 1073–1094.
Mitchell PW. 1980. The concepts defining the rate of swell of expansive soils. In *Proceedings of International Conference on Expansive Soils, ASCE* **1**: 22–28.
Nuhfer EB, Proctor RJ, Moser N. 1993. *The Citizen's Guide to Geologic Hazards*. AIPG Press: Arvada, CO; 134 pp.
Ritchie JT, Kissel DE, Burnett E. 1972. Water movement in undisturbed swelling clay. *Soil Science Society of America Journal* **36**: 874–879.
Ruan H, Illangasekare TH. 1998. A model to couple overland flow and infiltration into a macroporous vadose zone. *Journal of Hydrology* **210**: 116–127.
Russam K, Coleman JD. 1961. The effect of climatic factors on subgrade moisture condition. *Geotechnique* **3**: 22–28.
Smettem KRJ, Chillebrough DJ, Richards BG, Leaney FW. 1991. The influence of macropores on runoff generation from a hillslope soil with a contrasting textural class. *Journal of Hydrology* **122**: 235–252.
Stolte J, Ritsema CJ, Roo APJ. 1997. Effects of crust and cracks on simulated catchment discharge and soil loss. *Journal of Hydrology* **195**: 279–290.
USDA Soil Conservation Service. 1992. *State Soil Geographic Database (STATSGO) Data Users' Guide*. Publication no. 1492, US Government Printing Office; Washington, DC.
Van Stiphout TPJ, Van Laven HAJ, Boersma OH, Bouma J. 1987. The effect of bypass flow and internal catchment of rain on the water regime in a clay loam grassland soil. *Journal of Hydrology* **95**: 1–11.
Wise JR, Hudson WR. 1971. *An examination of expansive clay problems in Texas*. Center for Highway Research, Report No. 118–5, Austin, TX; 39 pp.
Wray WW. 1997. Using soil suction to estimate differential soil shrink or heave. In *Unsaturated Soil Engineering Practice*. *Geotechnical Special Publication* no. 68, ASCE.
Yaalon DH, Kalmar D. 1978. Dynamics of cracking and swelling clay soils: displacement of skeletal grains, optimum depth of slickensides, and rate of intra-pedonic turbation. *Earth Surface Processes* **3**: 41–42.

